ELSEVIER

Biophysical Chemistry 114 (2005) 35–41

Biophysical Chemistry

http://www.elsevier.com/locate/biophyschem

Dimethyl-pepep: a DNA probe in two-photon excitation cellular imaging

Alessandro Abbotto[a], Giancarlo Baldini[b], Luca Beverina[a], Giuseppe Chirico[b], Maddalena Collini[b,*], Laura D'Alfonso[b], Alberto Diaspro[c], Raffaella Magrassi[c], Luca Nardo[b], Giorgio A. Pagani[a]

[a]*Dipartimento di Scienza dei Materiali and INSTM, Università di Milano Bicocca, Italy*
[b]*INFM and Dipartimento di Fisica, Università di Milano Bicocca, Piazza della Scienza 3, 20126, Milano Italy*
[c]*INFM and Dipartimento di Fisica, Università di Genova, Italy*

Received 18 October 2004; accepted 4 November 2004
Available online 21 November 2004

Abstract

Dimethyl-pepep (D-pepep), a newly developed and very efficient two-photon absorber, has been tested here for two-photon excitation (TPE) cellular imaging. The spectral characteristics of the dye following one-photon excitation (OPE) and TPE (excitation and emission spectra, fluorescence lifetime, molecular brightness, saturation intensity) are reported. In vitro interaction studies with biomolecules show that dimethyl-pepep has a large affinity for DNA. A comparison with a widely used DNA stainer, 4-6-diamidino-2-phenylindole (DAPI) bound to DNA shows that the D-pepep brightness is one order of magnitude higher than that of DAPI, making this dye suitable for microscopy and imaging applications.

TPE images taken from double-stained yeast *Saccharomyces cerevisiae* cells have revealed that D-pepep localizes mainly in the nucleus, similarly to DAPI, and in mitochondria, although to a minor extent. Preliminary tests have shown that the dye cellular toxicity is negligible.

Keywords: Two-photon excitation microscopy; Fluorescence Imaging; DNA stainer

1. Introduction

Fluorescence microscopy, a widely adopted technique that can give details of a variety of physiological processes in the cell, offers enhanced resolution and high three-dimensional (3D) sectioning capabilities when coupled to confocal detection [1]. The visualization of specific physiological behaviors within the cell can be obtained by means of fluorophores which bind or diffuse to selected regions of the cell and which are sensitive to local environment changes, such as ion concentrations, or voltage drops across membranes. In the last decade, the two-photon excitation (TPE) microscopy has broken through the biomedical research with 3D optical sectioning capabilities similar to that of one-photon excitation (OPE) confocal microscopy and with conspicuous advantages for cellular applications, such as low Raman scattering, low autofluorescence background, and reduced out of focus bleaching [2].

In view of these applications, some of us have recently introduced a novel class of efficient heterocycle-based chromophores for two-photon absorption, with high quantum efficiency, large two-photon cross section and low bleaching rate [3]. By properly exploiting the relevant acceptor and donor properties of heterocyclic rings, such as pyridine and pyrrole, a number of dipolar [4,5], quadrupolar [6,7], and branched [8] two-photon absorbers were prepared and characterized in their linear and nonlinear optical properties. The two-photon absorption properties, both in the nanosecond (ns) and femtosecond (fs) regime, tell that [9] the two-photon absorption cross sections of the new dyes are among the largest ever

* Corresponding author. Tel.: +39 02 644 82871; fax: +39 02 644 2894.
E-mail address: Maddalena.collini@mib.infn.it (M. Collini).

0301-4622/$ - see front matter © 2004 Elsevier B.V. All rights reserved.
doi:10.1016/j.bpc.2004.11.004

reported for organic chromophores. Their two-photon-induced fluorescence emission has been reported [10,11] and, more recently, new isothiocyanate and maleimide derivatives for conjugation with biomolecules have been reported. The single-photon-induced fluorescence in cells and cell toxicity of many members of the heterocycle-based TPA series is under active investigation.

We give here a detailed characterization of the most representative system of the quadrupolar series, dimethyl-pepep (D-pepep) [6,7], in view of cellular imaging applications. Its measured (Z-scan) two-photon absorption cross section in dimethyl-sulfoxide (DMSO) solution is 347 GM at 707 nm upon femtosecond excitation [6,7,9] (where 1 Göppert–Mayer=1×10^{-50} cm^4 s $photon^{-1}$ $molecule^{-1}$). This dye has a fluorescence brightness (defined as absorption cross section times quantum yield) comparable to that of fluorescein or rhodamine [12].

Here, we report some relevant spectral characteristics of the dye upon two-photon excitation such as excitation and emission spectrum, fluorescence lifetime, and molecular brightness.

In vitro interaction studies on selected biomolecules, such DNA from calf thymus and bovine serum albumin (BSA), show that dimethyl-pepep has a pronounced affinity for DNA, with values close to those found for 4-6-diamidino-2-phenylindole (DAPI) and ethidium bromide. On the contrary, a modest binding is found bovine serum albumin (BSA).

In order to confirm the dye affinity for DNA in vivo, imaging studies have been performed on cells of yeast *Saccharomyces cerevisiae* labeled with D-pepep. A quantitative comparison on yeast cells stained also with DAPI shows that the two dyes diffuse in similar region of the cell, although D-pepep has a larger brightness.

This work is aimed to enlighten the D-pepep properties compared to that of one of the best known and widely used stainer, such as DAPI, and it is not meant to be an exhaustive screening of the properties of existent DNA stainers.

2. Materials and methods

2.1. Materials

Dimethyl-pepep (D-pepep, Scheme 1) has been synthesized as previously described [6,7]. Rhodamine 6G has been purchased by Fluka Chemical, calf thymus DNA, and Bovine Serum Albumin (BSA) were purchased by Sigma-Aldrich Chemical. All reagents [ethanol, dimethyl-sulfoxide (DMSO)] were of the highest purity. D-pepep was dissolved in DMSO in order to obtain a millimolar stock, then diluted in the proper solvent (ethanol or buffer) just before each measurements. Rhodamine 6G was dissolved in ethanol, while the biological samples were dissolved in the proper buffer, usually a phosphate buffer at pH 7.5 at the desired ionic strength. Solution concentrations were checked photometrically by employing the proper molar extinction coefficients according to: ε(525 nm)=72,000 M^{-1} cm^{-1} for D-pepep in DMSO, ε(525 nm)=96,000 M^{-1} cm^{-1} for rhodamine in ethanol, ε(260 nm)=6600 M^{-1} cm^{-1} for calf thymus DNA, ε(280 nm)=44,000M^{-1} cm^{-1} for BSA, respectively.

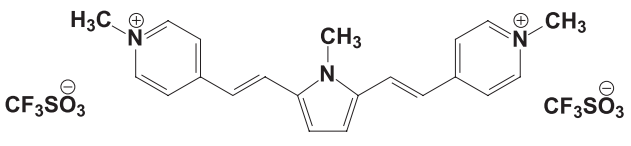

Scheme 1. Dimethyl-pepep: chemical structure.

Yeast *S. cerevisiae* cells have been stained with D-pepep or with DAPI starting from 10-μM stock solutions with incubation times ranging from 10 to 40 min. Control (unstained) cells were also prepared in order to estimate the autofluorescence contribution.

Citotoxicity measurements have been performed on Chinese Hamster Ovary (CHO) cells grown in a complete culture medium (MEM+2 mM glutammine–gentomicin+10% fetal bovine serum). Their vitality has been monitored by Trypan Blue (1:2) [13]. During the experiments, the cells have been kept under usual culture condition (5% CO_2, 37 °C). D-pepep has been dissolved directly in phosphate buffer, then filtered and diluted up to 40 μM, the final incubation concentration being about 4 μM. Cells counting has been accomplished by a Toma's chamber. Every count has been repeated at least three times for each incubation time, and the units of the total number of cells is given per milliliter. All the counts have been performed when the culture flasks of the cells had been splitted by 0.25% of trypsin–EDTA solution, centrifuged at 2000 rpm for 5 min, and resuspended in the complete medium.

2.2. Techniques

Steady state fluorescence measurements and the fluorescence titrations of D-pepep and DNA have been performed on a Cary Eclipse spectrofluorimeter (Varian, Victoria, Australia), exciting the dye at 525 nm.

Fluorescence lifetime measurements have been performed on a multifrequency phase fluorometer (K2, ISS, Urbana, IL), employing either the output 514-nm line of an Argon ion continuous wave laser (2025, Spectra Physics, Mountain View, CA) or the 790-nm output of a mode-locked Ti:Sapphire (Tsunami3960, Spectra Physics) pumped by a solid state laser at 532 nm (Millenia V, Spectra Physics). The temporal characteristics of the beam were 80 fs of pulse width and 80 MHz of repetition rate. Tsunami output, properly attenuated with neutral density filters, is coupled to an inverted microscope (TE300, Nikon, USA) in the epifluorescence setup. An oil-immersion objective at high numerical aperture

(Nikon, 100×, NA=1.3) has been used. The pulse width increases to 150 fs in the focal plane. A dichroic mirror (650 DCSPRX C72-38; Chroma, Brattelboro, VT) coupled to a short pass filter allows to send the fluorescence signal to the lateral exit of the microscope where a homemade housing allows to align two channels, Avalanche Photo Diode (APD) detectors or a photomultiplier tube. In order to select D-pepep emission, a 600-nm band pass filter (fwhm=40 nm, Chroma Technologies, Brattelboro, VT) was used at the entrance of the detector channel. The two-photon emission spectrum has been acquired by putting a monochromator (Jobin-Ivon) in place of the band-pass filter.

For the photon counting histogram (PCH) measurements, the APD detector output was connected to an analog–digital I–O board (PCI 6711, National Instruments, Mountain View, CA). PCH were acquired for 120 s at a sampling rate of 10 kHz, thereby obtaining histograms over 1,200,000 data points. From test measurements on diluted rhodamine 6G solutions we have estimated V_{EXC}=0.2 μm^3 at λ=790 nm. We have employed here the moment analysis of the photon counting histogram (PCH) technique in order to obtain an estimate of D-pepep molecular brightness ε and of the average number of fluorophores in the excitation volume, N_{EXC}. This analysis is based on the measurement of the first two moments of the number of fluorescence photoelectrons per sampling time, $\langle k\rangle$ and $\langle k^2\rangle$, according to [14]:

$$\langle k\rangle = \varepsilon N_{EXC} \quad \left(\left\langle k^2\right\rangle - \langle k\rangle^2\right)\Big/\langle k\rangle = 1 + \gamma\varepsilon \qquad (1)$$

where γ is a numerical factor (γ=0.076 for TPE).

TPE images have been acquired by coupling the two-photon excitation source (Tsunami, Spectra Physics) to the Nikon TE300 inverted microscope through a PCM2000 Nikon scanning head [15]. The residence time of each acquisition and the photomulitplier (PMT) gain were adjusted properly in order to obtain a good signal to noise ratio. The axial and lateral resolution of the system are 800 and 250 nm, respectively [16]. The image analysis and visualization were performed using a home-coded software and EZ2000 platform (Nikon, NL).

3. Results and discussion

3.1. Spectral properties

D-pepep has a high one-photon excitation (OPE) extinction coefficient at 525 nm of 72,000±3500 M^{-1} cm^{-1} in dimethyl-sulfoxide (the value remains similar in ethanol, whereas in phosphate buffer at pH 7, it decreases at 52,000±3000 M^{-1} cm^{-1}). In panel A of Fig. 1, the OPE excitation and emission spectra of D-pepep in different solvents are shown. The fluorescence emission peaks at

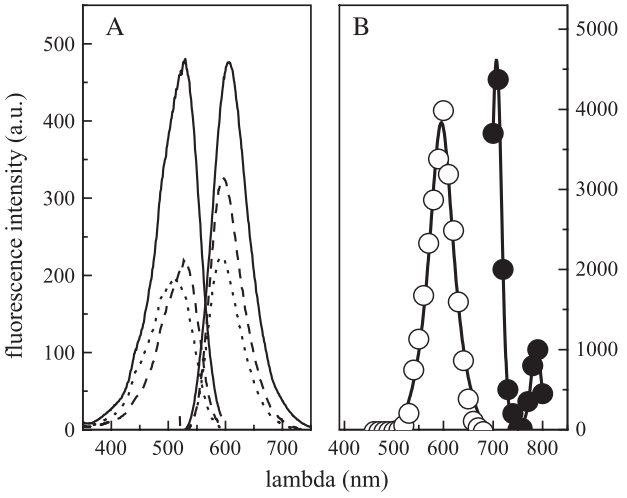

Fig. 1. Panel A. One-photon excitation (OPE) excitation and emission spectra in different solvents: DMSO, continuous line; ethanol, dashed line; phosphate buffer at pH 7, dotted line. Panel B. Two-photon excitation (TPE) excitation (●) and emission (○) spectra of D-pepep in buffer solution.

≈600 nm. Its fluorescence quantum yield is ≈0.3 in DMSO, ≈0.15 in ethanol and ≈0.1 in buffered solution at pH 7 [10,11].

The probe has a large two-photon cross section, about 347 GM at 707 nm, which decreases to 112 GM at 790 nm [9]. This trend is confirmed by the two-photon excitation (TPE) spectrum of D-pepep in ethanol measured here which shows a main peak at 720 nm and a secondary one at about 790 nm (Fig. 1, panel B). The TPE emission spectrum is not appreciably different from that obtained with one-photon excitation [10]. Similarly, the fluorescence lifetime values of D-pepep do not change upon OPE or TPE. In particular, it is found that D-pepep decays as a single exponential in pure solvents, such as DMSO, where $\tau \approx 1.50 \pm 0.05$ ns, in ethanol where $\tau \approx 1.05 \pm 0.05$ ns, and in water, phosphate buffer (pH=7), where $\tau \approx 0.60 \pm 0.03$ ns.

From the data illustrated above, it can be evinced that D-pepep spectral properties, such as the absorption peak wavelength, the oscillator strength, the emission quantum efficiency, and the fluorescence lifetime, have been found to depend upon solvent polarity.

3.2. TPE response

D-pepep fluorescence versus laser power follows initially the expected quadratic dependence (inset of Fig. 2, panel A) until saturation occurs. In order to determine the power value for saturation, P_{sat}, a fit of the fluorescence signal F versus laser power has been performed according to the expression [17]

$$F = A\frac{P^2}{1 + (P/P_{sat})^2} \qquad (2)$$

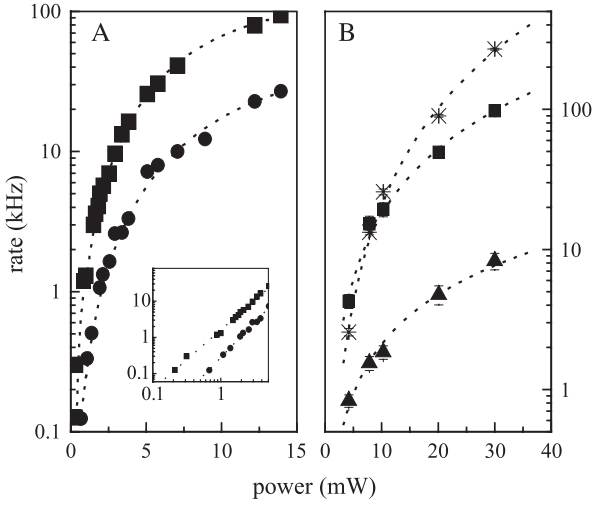

Fig. 2. Panel A. Fluorescence intensity, counting rate, kHz, versus the laser power in mW at 790 nm of 100 nM D-pepep in ethanol (■) and in buffer (●) solution. The data are fitted according to Eq. (2) (continuous line). Inset of panel A: zoom of the initial quadratic power law region in double logarithmic plot of the same data of panel A. Panel B. Fluorescence counting rate, kHz, for D-pepep–DNA (■), DAPI–DNA (▲) and rhodamine 6G (*) versus laser power in mW at 720 nm. The dyes concentration was 0.2 μM and the DNA concentration was 200 μM. The solid lines are the fits by means of Eq. (2).

where A is a constant that contains the dependence upon the cross section and the quantum yield. We find P_{sat}=16 mW, corresponding to $I_{sat} \cong 3.2$ MW/cm^2 and P_{sat}=10 mW, corresponding to $I_{sat} \cong 2.2$ MW/cm^2 for ethanol and water, respectively.

TPE molecular brightness, given by the product of the TPE cross section, the quantum yield, and the excitation intensity, is the parameter that is actually determining the possibility to employ this dye for TPE microscopy. The brightness can be estimated by performing PCH measurements on an ethanol solution of D-pepep at a concentration of 100 nM, comparing this value with a solution of a commonly used bright dye for two-photon excitation, rhodamine 6G at the same concentration. The molecular brightness of D-pepep, in the quadratic power dependence regime, has been found to be about one third that of rhodamine 6G, thereby showing that this dye can be successfully used with TPE [18].

3.3. In vitro interaction studies

In order to test the affinity of D-pepep for biomolecules, we have performed some in vitro interaction studies with model macromolecules, calf thymus DNA, and bovine serum albumin. Fig. 3 shows the fluorescence titrations of D-pepep calf thymus DNA at three ionic strengths. A fluorescence enhancement is found upon binding and, by exploiting the different response of DNA bound and free dye, we extract the binding constant for the association reaction. In fact, the total fluorescence intensity, F, can be expressed as a linear combination of the free (η_F) and bound (η_B) quantum efficiencies weighted on the respective concentrations, c_B and c_F.

$$F = \eta_B c_B + c_F \eta_F \tag{3}$$

The binding curves have been fitted to a standard independent sites model isotherm [19] given by the mass law: $c_F + (P)_0 \Leftrightarrow c_B$ where $(P)_0 = nP - c_B$ are the free DNA sites, n is the number of sites on DNA available to the dye, P is the total DNA concentration. The association constant K is then given by:

$$K = c_B / [(nP - c_B) c_F]. \tag{4}$$

A simple inversion of Eq. (4) yields directly the concentration of bound ligand versus K, n, and the total ligand $c_T = c_B + c_F$ and macromolecule in solution, according to:

$$2c_B = (K^{-1} + nP + c_T) - \sqrt{(K^{-1} + nP + c_T)^2 - 4nPc_T}. \tag{5}$$

At 100 mM ionic strength, the measured association constant is $2.0 \pm 0.5 \times 10^6$ M^{-1}. This value is of the same order of magnitude reported for other dyes, such as ethidium bromide or DAPI for calf thymus DNA [20,21]. The relatively large value of the number of base pair per site found for D-pepep, $n = 13 \pm 2$, suggests that this dye could be a minor groove binder, such as netropsin, Hoechst 33258 [22], and, in some cases, DAPI [21]. Further investigation to this point is currently in progress.

Since the D-pepep is dicationic, ionic strength is expected to influence the binding process through electrostatic contribution, and, in fact, the observed equilibrium constant decreases with increasing salt concentration yielding values of the association constant given by:

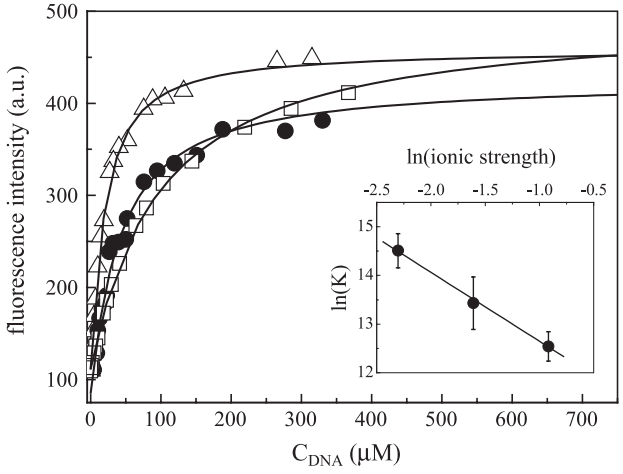

Fig. 3. Fluorescence titrations of D-pepep with calf thymus DNA at different ionic strength versus DNA concentration. D-pepep was excited at 525 nm and the emission was followed at 610 nm. Symbols refer to different ionic strengths: 100 mM, △; 200 mM, ●; and 400 mM, □. The titrations have been fitted according to Eq. (5) (solid lines). The inset shows the affinity constants versus ionic strength in a double logarithm plot.

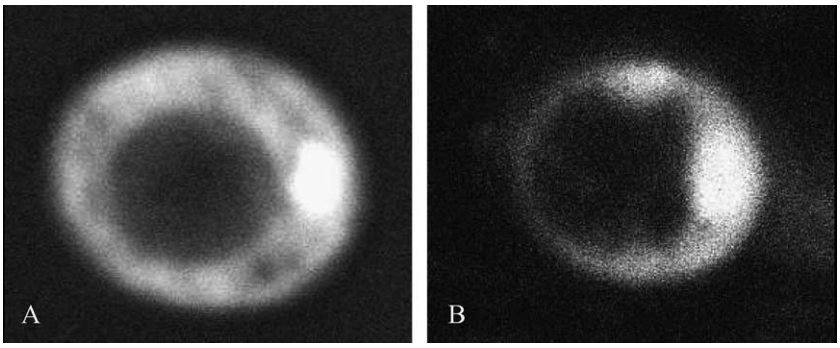

Fig. 4. TPE images of yeast stained cells taken at 790 nm, 2 mW of laser power. Each image is the average of 10 images with a pixel size of 34 nm. Panel A. D-pepep-stained cell; Panel B. DAPI-stained cell. In both stained cells, the nucleus and the mithocondrial DNA are visible near the cell membrane.

$6.8\pm0.5\times10^5$ M^{-1} at 200 mM and $2.8\pm0.5\times10^5$ M^{-1} at 400 mM. In particular, following the predictions from the ion-condensation theory for polyelectrolytes [23], log$K$ versus log(ionic strength) is expected to be given by a straight line. As shown in the inset of Fig. 3, we find a linear dependence with a slope $m=1.1\pm0.3$, thus suggesting that only one charge only of the probe affects the binding to DNA.

When D-pepep is bound to DNA, its fluorescence quantum yield increases almost fourfold (quantum yield of $\cong0.1$ in buffer to $\cong0.4$ when bound to DNA) and the response of the bound dye is found to be similar at the different ionic strengths, within experimental error (typically 10% at most).

The fluorescence enhancement is also confirmed by the increase of the D-pepep fluorescence lifetime from 0.6 ± 0.1 ns (free) up to 2.0 ± 0.3 ns (bound), suggesting that the bound dye has a higher degree of shielding from the solvent.

In order to quantify the brightness enhancement of D-pepep upon binding, we have followed the emission rate of the dye bound to calf thymus DNA versus excitation power comparing this signal both to that obtained from rhodamine 6G in ethanol, and from the DAPI–DNA complex. DAPI has been chosen since it is a widely used and well-characterized in vitro and in vivo DNA stainer [20,21] to which other DNA ligands for microscopy have been compared. The fluorescence signal versus excitation power has been recorded both at 790 nm (data not shown) and at 720 nm (shown in Fig. 2B) where free DAPI TPE cross section is largest (about 0.16 GM). The concentration of the dyes was 0.2 μM, and the DNA concentration was 200 μM, thus ensuring that almost all the dye was bound, as it can be estimated from the values of the association constants. Fig. 2 shows that D-pepep bound to DNA has a brightness about one order of magnitude larger than that of bound DAPI, and that its brightness is comparable to that of rhodamine in the quadratic range of power law dependence (15 mW).

D-pepep titrations were performed also with bovine serum albumin, a protein that has several hydrophobic pockets suitable for small ligand binding [24]. In this case, however, we find a very low binding affinity for BSA, with association constant lower than 10^2 M^{-1}. This finding indicates that the interaction of D-pepep with biomolecules is not only driven by hydrophobic forces, but a significant contribution from electrostatic forces occurs.

3.4. In vivo interaction studies

In vivo studies have been performed by incubating *S. cerevisiae* cells with D-pepep, at concentrations ranging 1–10 μM. The cells are found to be permeable to this dye

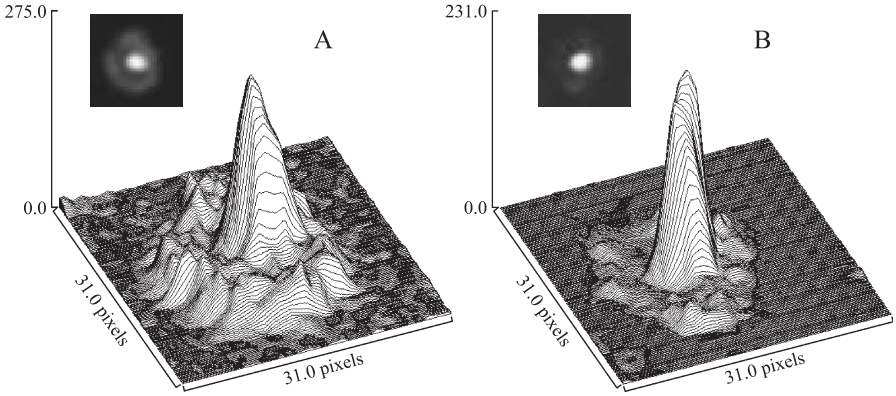

Fig. 5. Colocalization images from doubly stained yeast cells taken at 720 nm, 500 μW laser power. Panel A. 3D-contour plot of D-pepep emission selected trough a 600/40 nm band-pass filter. Panel B. 3D-contour plot of DAPI emission selected trough a 485/30 nm band-pass filter. The inset in each contour plot is a 6×6 μm portion of the 30×30 μm original image with 200 nm of pixel size.

in about 15–20 min. Fluorescence imaging has been employed in order to follow the distribution of D-pepep in the cells. The TPE brightness of the dye is sufficient to collect fluorescence images with dwell times as short as ≅10 μs and excitation powers as low as ≅2 mW at 790 nm (objective NA=1.3). In panel A of Fig. 4, an image of a D-pepep-stained yeast cell (pixel size=34×34 nm^2, average of 10 images, band-pass filter 600/40 nm) is shown. An image of an unstained cell taken under the same experimental conditions (data not shown) shows that the cell autofluorescence is very low in the spectral region of D-pepep emission. For comparison, yeast cells have been stained also with the same concentration of DAPI (Fig. 4, panel B, same pixel size, band-pass filter 485/30 nm). Fig. 4 shows that both dyes diffuse in DNA-rich regions, such as the nucleus and the mithocondria. The affinity of D-pepep for cellular DNA is also confirmed by D-pepep and DAPI colocalization measurements, as shown in the 3D contour plot Fig. 5. Nominal dye concentrations were 0.3 μM for D-pepep and 0.8 μM for DAPI. The images were acquired at a laser power of 500 μW at 720 nm. A 50% beam splitter coupled to a 600/40 nm and to a 485/30 nm band-pass filter in front of two APDs has been used to simultaneously acquire the images. The original image is shown on the left side of each contour plot, and it is a 6×6 μm portion of a 30×30 μm larger image with 200 nm of pixel size. The 3D plots show that the maximum fluorescence for the double-stained yeast cells is observed in the nucleus for both dyes, but D-pepep also significantly stains the mithocondrial regions. Since DAPI is about threefold more concentrated in the cell than D-pepep, the higher fluorescence signal found for D-pepep strongly indicates that D-pepep is a more efficient dye for TPE microscopy.

More quantitatively, it is possible to estimate the population and brightness of D-pepep in different cell compartments by means of PCH measurements. We have found that the highest D-pepep concentration is found in the cell nucleus but also the mithocondrial DNA gives an appreciable contribution to the fluorescence signal. In particular, the ratio of the number of D-pepep molecules per excitation volume in the nucleus to that measured in mithocondria is about 7±2 whereas the brightness is very similar in the two cell compartments, about 4.0±0.5 kHz at 1 mW of laser power, well below saturation threshold.

3.5. Cell toxicity

A preliminary study has been undertaken in order to test D-pepep toxicity on standard cells from Chinese Hamster Ovary (CHO). The cells were incubated with 4 μM of D-pepep for 2, 4, 8 h, and overnight. Control cells, to which the same buffer volume has been added, were counted at 0, 2 h, and overnight. The results of the different counts, shown in Table 1, indicate that the ratio of living to the dead cells is independent of incubation time and of the addition of the dye (but depends probably on tripsinization), thereby suggesting that D-pepep is not appreciably citotoxic for CHO cells.

Table 1
Effect of D-pepep on CHO cells at different incubation times

Incubation time	HCO + D-pepep (cells/ml)		Control HCO (cells/ml)	
	Alive	Dead	Alive	Dead
0 h	–	–	2.2×10^5	2.0×10^4
2 h	3.2×10^5	2.0×10^4	1.9×10^5	2.0×10^4
4 h	2.8×10^5	2.0×10^4	–	–
8 h	1.2×10^5	2.0×10^4	–	
Overnight	1.6×10^5	2.0×10^4	1.8×10^5	2.0×10^4

In conclusion, a relevant result of this preliminary characterization comes from imaging experiments on cells, where D-pepep has proved to be a very efficient dye for two-photon excitation microscopy. It has to be noted that the fairly high quantum efficiency of DNA–D-pepep complex and the high affinity for cellular DNA makes it a valuable DNA stainer also in confocal microscopy due to its visible (525 nm) absorption peak that can be excited by Argon laser sources [15].

Acknowledgements

This work has been partially supported by MURST-Cofin 2002 and INFM PAIS MEAB. Thanks are due to Michele Caccia for his help in PCH measurements.

References

[1] A. Diaspro, G. Chirico, Two-photon excitation microscopy, Adv. Imaging Electron Phys. 126 (2003) 195–286.
[2] K. Koenig, U.K. Tirlapur, Cellular and subcellular perturbations during mutliphoton microscopy, in: A. Diaspro (Ed.), Confocal and Two-photon Microscopy, Wiley, New York, 2002.
[3] C. Xu, Cross-sections of fluorescent molecules in multiphoton microscopy, in: A. Diaspro (Ed.), Confocal and Two-photon Microscopy, Wiley, New York, 2002.
[4] A. Abbotto, L. Beverina, R. Bozio, S. Bradamante, C. Ferrante, G.A. Pagani, R. Signorini, Push–pull organic chromophores for frequency-upconverted lasing, Adv. Mater. 12 (2000) 1963–1967.
[5] A. Abbotto, L. Beverina, R. Bozio, S. Bradamante, G.A. Pagani, R. Signorini, Heterocycle-based materials for frequency-upconverted lasing, Synth. Met. 121 (2001) 1755–1756.
[6] A. Abbotto, L. Beverina, R. Bozio, A. Facchetti, C. Ferrante, G.A. Pagani, D. Pedron, R. Signorini, Novel heterocycle-based two-photon absorbing dyes, Org. Lett. 4 (2002) 1495–1498.
[7] A. Abbotto, L. Beverina, R. Bozio, S. Bradamante, A. Facchetti, C. Ferrante, G.A. Pagani, D. Pedron, R. Signorini, Novel heterocycle-based two-photon absorbing dyes, NATO Sci. Ser., II 100 (2003) 385–393.
[8] A. Abbotto, L. Beverina, R. Bozio, A. Facchetti, C. Ferrante, G.A. Pagani, D. Pedron, R. Signorini, Novel heteroaromatic-based multi-branched dyes with enhanced two-photon absorption activity, Chem. Commun. 17 (2003) 2144–2145.
[9] R. Signorini, C. Ferrante, D. Pedron, M. Slaviero, R. Bozio, L. Beverina, A. Abbotto, G.A. Pagani, Highly efficient multiphoton

absorption in a new quadrupolar heterocyclic dye, NATO Sci. Ser., II 100 (2003) 231–240.
[10] A. Abbotto, L. Beverina, G. Chirico, A. Facchetti, P. Ferruti, M. Gilberti, G.A. Pagani, Crosslinked poly(amido-amine)s as superior matrices for chemical incorporation of highly efficient organic nonlinear optical dyes, Macromol. Rapid Commun. 24 (2003) 397–402.
[11] A. Abbotto, L. Beverina, G. Chirico, A. Facchetti, P. Ferruti, G.A. Pagani, Design and synthesis of new functional polymers for nonlinear optical applications, Synth. Met. 139 (2003) 629–632.
[12] A. Abbotto, L. Beverina, G.A. Pagani, M. Collini, G. Chirico, L. D'Alfonso, G. Baldini, Novel efficient and stable heteroaromatic two-photon absorbing dyes, Proc. SPIE 5139 (2003) 223–230.
[13] S.E. Murinda, K.A. Rashid, R.F. Roberts, In vitro assessment of the cytotoxicity of nisin, pediocin, and selected colicins on simian virus 40-transfected human colon and Vero monkey kidney cells with trypan blue staining viability assays, J. Food Prot. 66 (2003) 847–853.
[14] Y. Chen, J.D. Muller, P.T.C. So, E. Gratton, The photon counting histogram in fluorescence fluctuation spectroscopy, Biophys. J. 77 (1999) 553–567.
[15] A. Esposito, F. Federici, C. Usai, F. Cannone, G. Chirico, M. Collini, A. Diaspro, Notes on theory and experimental conditions behind two-photon excitation microscopy, Microsc. Res. Tech. 63 (2004) 12–17.
[16] A. Diaspro, G. Chirico, F. Federici, F. Cannone, S. Beretta, Two-photon microscopy and spectroscopy based on a compact confocal scanning head, J. Biomed. Opt. 6 (2003) 300–310.
[17] J. Mertz, Molecular photodynamics involved in multi-photon excitation fluorescence microscopy, Eur. Phys. J., D At. Mol. Opt. Phys. 3 (1998) 53–66.
[18] P. Schwille, U. Haupts, S. Maiti, W.W. Webb, Molecular dynamics in living cells observed by fluorescence correlation spectroscopy with one- and two-photon excitation, Biophys. J. 77 (1999) 2251–2265.
[19] C.R. Cantor, P.R. Schimmel, Biophysical Chemistry, W.H. Freeman & Co., San Francisco CA, 1980.
[20] W.D. Wilson, F.A. Tanious, H.J. Barton, R.L. Jones, K. Fox, R.L. Wydra, L. Strekowski, DNA sequence dependent binding modes of 4′,6′-diamino-2-phenylindole (DAPI), Biochemist 29 (2003) 8452–8461.
[21] F.A. Taniuos, J.M. Veal, H. Buczak, L.S. Ratmeyer, W.D. Wilson, DAPI (4′,6′-diamino-2-phenylindole) binds differently to DNA and RNA: minor-groove binding at AT sites and intercalation at AU sites, Biochemist 31 (1992) 3103–3112.
[22] F.G. Loontiens, L.W. McLaughlin, S. Diekmann, R.M. Clegg, Binding of hoechst 33258 nd 4′-6′-diamino-2-phenylindole to self-complementary decadeoxynucleotides with modified exocyclic base substituents, Biochemist 30 (1991) 182–189.
[23] G.R. Manning, The molecular theory of polyelectrolyte solutions with applications to the electrolyte properties of polynucleotides, Q. Rev. Biophys. 11 (1978) 178–246.
[24] D. Matulis, C.G. Baumann, V.A. Bloomfield, R.E. Lovrien, 1-Anilino-8-naphthalene sulfonate as a protein conformational tightening agent, Biopolymers 49 (1999) 451–458.